Topology Optimization of Manifold Microchannel Heat Sinks

Yuqing Zhou* §, Tsuyoshi Nomura* † and Ercan M. Dede*
*Toyota Research Institute of North America, Ann Arbor, MI, USA
†Toyota Central R & D Labs., Inc., Yokomichi, Nagakute, Japan
§Corresponding author: yuqing.zhou@toyota.com

***Abstract*—The manifold microchannel (MMC) heat sink has been widely studied for liquid-cooling of power-dense electronic components. Conventionally, thermal-fluid performance of an MMC heat sink is analyzed via unit cell simulations and designed by varying the rectangular fin and channel geometries, namely size optimization. To further explore the performance potential of the MMC heat sink, this paper proposes topology optimization (TO) to design the optimal freeform fin/channel geometry to maximize heat transfer performance while minimizing the required pumping power. The heat transfer physics in an MMC heat sink is governed by conjugate heat transfer between an incompressible laminar fluid and a heated conductor. The MMC heat sink fin/channel geometry design is formulated as a material distribution problem in a periodic unit cell. Since TO describes the geometry non-parametrically, it facilitates innovative designs through the exploration of arbitrary shapes. The physics-governed design optimization problem is solved by mathematical programming using design sensitivities and an iterative gradient-based method. The thermal-fluid performance is presented for both conventional size optimization and the proposed TO approach, considering the heat transfer performance versus the required pumping power. It is demonstrated that the TO designed fin/channel geometries outperform those obtained through size optimization. Due to the shape complexity associated with the TO designed fin/channel geometries, they are not readily suitable for conventional manufacturing processes, *e.g.*, machining and metal die-casting. However, such out-of-box designs fully exploit the flexibility offered by the latest advanced manufacturing processes, *e.g.*, additive manufacturing and rapid investment casting.**

***Index Terms*—topology optimization, conjugate heat transfer, manifold microchannel heat sink, additive manufacturing**

I. Introduction

Power electronics circuits are widely used in automotive, data center, aerospace and distributed energy or grid applications. Due to the trending demand for high efficiency, integrated-functionality and a compact form factor, the power density of power electronics circuits has been inevitably increasing. As a result, the thermal management of such power-dense systems requires higher heat dissipation while balancing pumping power requirements. Innovative cooling solutions have been proposed to address this challenge, *e.g.*, microchannel heat sinks [1], two-phase flow with boiling [2], and the use of nanofluid coolants [3]. This paper focuses on manifold microchannel (MMC) heat sink technology, which differs from a traditional microchannel heat sink by introducing an additional manifold component to navigate coolant flow perpendicular to the microchannel structure through alternating or interleaved inlet and outlet branches. By distributing the coolant flow before it enters the microchannel unit cell, both the system pressure loss (*i.e.*, pumping power requirement) and the temperature variation on the base plate can be significantly reduced at the expense of some slight increase of the packaging form factor due to the added manifold component. Figure 1 shows a representative MMC heat sink assembly. The coolant flow path within the manifold insert plus microchannels is demonstrated in Fig. 2, where blue colored and red colored arrows, respectively, denote cold and hot coolant fluid streams.

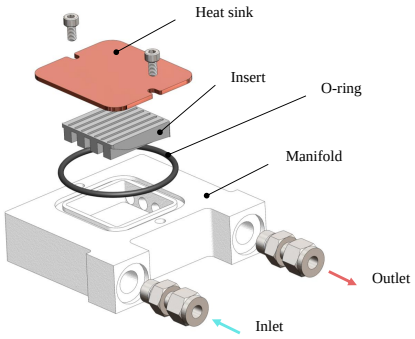

Fig. 1. Exploded assembly view of a representative MMC heat sink assembly.

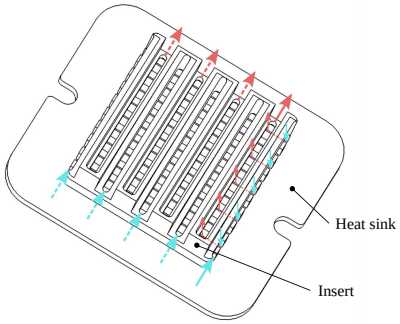

Fig. 2. Coolant flow path within the manifold insert and microchannels in a conventional MMC heat sink with straight rectangular fins. Blue colored arrows indicate low-temperature fluid flow before it enters the microchannel unit cells. Red colored arrows indicate heated high-temperature flow after the fluid exits the unit cells.

Since the introduction of the MMC heat sink [4], extensive investigation has been conducted regarding its computational

analysis [5], experimental validation [6] and performance optimization [7], [8]. However, only straight rectangular fin geometries have been studied for MMC heat sinks. This paper applies topology optimization (TO) to further explore the thermal-fluid performance potential of MMC heat sinks.

TO is a computational synthesis approach that explores the optimal geometries for physics (or multiphysics) governed systems. The geometry exploration is formulated as a material distribution design problem. Since the concept of TO was first proposed [9] using a homogenization method for structural mechanics, alternative methods (*e.g.*, SIMP [10], [11], ESO [12], level-set [13], [14]) have been developed and applied to various applications (*e.g.*, fluidics [15], photonics [16], electromagnetics [17] and acoustics [18]). This paper focuses on conjugate heat transfer TO using a density-based method. In the density-based TO method [19], the free-form geometry design is modeled by nodal design variables. While continuous values (*i.e.*, "blurry" geometry) are allowed during the course of optimization, discrete convergence (*i.e.*, "crisp" geometry) is encouraged via interpolation functions and achieved via iterative gradient-based methods at the end of the optimization. In the case of fin/channel geometry design, a design value of 0 indicates solid walls, while a value of 1 indicates fluid channels. Following pioneering work in conjugate heat transfer TO [20], [21], the method has been applied to the design of air-cooled heat sinks [22]–[24] and liquid-cooled heat sinks [25]–[33]. This paper presents, for the first time, the use of conjugate heat transfer TO for the design of three-dimensional (3-D) MMC heat sinks, while related works all used traditional (manifold-less) microchannel heat sink configurations with limited 3-D attempts.

To demonstrate the thermal-fluid performance improvement, the novel fin/channel designs obtained by TO are benchmarked against conventional straight rectangular fin designs. The numerical results reveal that the TO designed fin/channel geometries outperform conventional straight rectangular fin designs (heat dissipation capability versus pumping power requirement). It is acknowledged that the shape complexity associated with the TO designed fin/channel geometries is apparently not suitable for conventional manufacturing processes, *e.g.*, machining and metal die-casting. However, such out-of-box designs fully exploit the flexibility offered by latest advanced manufacturing processes, *e.g.*, additive manufacturing and rapid investment casting.

II. Method

The proposed method including design variable description, governing equations, optimization objective function plus formulation, and numerical implementation are described in this section.

A. Design Variable

In a prescribed, fixed design domain, D, a characteristic function, χ, is defined to describe the channel domain, Ω_c, to be optimized:

$$\chi(\mathbf{x}) = \begin{cases} 0 & \text{for} \quad \forall \mathbf{x} \in D \setminus \Omega_c \\ 1 & \text{for} \quad \forall \mathbf{x} \in \Omega_c \end{cases}, \tag{1}$$

where $\mathbf{x}$ stands for a design point in D, and $\chi(\mathbf{x})$ is defined by a scalar function, ϕ, and a Heaviside function, H, such that:

$$\chi(\mathbf{x}) = H\left(\phi(\mathbf{x})\right) = \begin{cases} 0 & \text{for} \quad \forall \mathbf{x} \in D \setminus \Omega_c \\ 1 & \text{for} \quad \forall \mathbf{x} \in \Omega_c \end{cases}. \tag{2}$$

A Helmholtz partial differential equation (PDE) filter [34], [35] is introduced to regularize ϕ:

$$-R_\phi^2 \nabla^2 \tilde{\phi} + \tilde{\phi} = \phi, \tag{3}$$

where R_ϕ is the filter radius. Then, the regularized nodal design variable, γ, is defined by an additional smoothed Heaviside function, $\tilde{H}$:

$$\gamma = \tilde{H}(\tilde{\phi}). \tag{4}$$

After the regularization, $\phi \rightarrow \tilde{\phi} \rightarrow \gamma$, the resulting regularized nodal design variable, γ, is bounded between 0 and 1, where $\gamma = 0$ indicates solid material walls and $\gamma = 1$ indicates fluid flow channels. In a practical optimization formulation, the original nodal design variable, ϕ, is bounded between -1 and 1.

B. Governing Equations

In an MMC heat sink, the heat transfer physics is governed by conduction in a solid plus convection via a surrounding fluid medium. Such phenomenon is often regarded as conjugate heat transfer.

The equilibrium equations governing the flow physics (assuming incompressible laminar flow in porous media) is summarized as follows:

$$\begin{aligned} \rho(\mathbf{u} \cdot \nabla)\mathbf{u} &= -\nabla p + \nabla \cdot \left(\mu \left(\nabla \mathbf{u} + (\nabla \mathbf{u})^\intercal\right)\right) - \mu\alpha(\gamma)\mathbf{u}, \\ \nabla \cdot (\mathbf{u}) &= 0, \end{aligned} \tag{5}$$

where ρ is the fluid density, $\mathbf{u}$ is the fluid velocity vector (state variable), p is the pressure (state variable), μ is the fluid dynamic viscosity, and $\alpha(\gamma)$ is the effective inverse permeability, which is a function of the regularized design variable, γ.

The effective inverse permeability interpolation function is defined as follows [36]:

$$\alpha\left(\gamma\right) = \alpha_{\text{min}} + \left(\alpha_{\text{max}} - \alpha_{\text{min}}\right) \frac{q_\alpha(1-\gamma)}{q_\alpha + \gamma}. \tag{6}$$

As γ approaches 0, $\alpha\left(\gamma\right)$ approaches α_{max} indicating a low permeability quasi-solid state. As γ approaches 1, $\alpha\left(\gamma\right)$ approaches α_{min} indicating a fluid state. In this expression, q_α is a tuning parameter controlling the function convexity.

The equilibrium equation governing the heat conduction and convection physics is summarized as follows:

$$\rho C_p \mathbf{u} \cdot \nabla T = \nabla \cdot \left(k\left(\gamma\right) \nabla T\right) - Q, \tag{7}$$

where C_p is specific heat capacity, T is the temperature (state variable), Q is the volumetric heat generation, and $k(\gamma)$ is the effective thermal conductivity, which is a function of the regularized design variable, γ.

The effective thermal conductivity interpolation function is defined as follows [37]:

$$k(\gamma) = \frac{\gamma\left(C_k(1+q_k)-1\right)+1}{C_k(1+q_k\gamma)}, \tag{8}$$

where

$$C_k = \frac{k_f}{k_s}. \tag{9}$$

k_f is the thermal conductivity of the assumed fluid, k_s is the thermal conductivity of the assumed solids, and q_k is another tuning parameter controlling the function convexity.

Note that for the material properties assumed in this study, the product of ρC_p on the left-hand-side of (7) is approximately constant. Thus, density and specific heat are not interpolated in this work.

C. Objective Function

A multi-objective function is defined as a weighted linear combination of flow resistance, f_1, and average temperature at the base plate, f_2, following a similar approach in [20]:

$$f = w_1 f_1 + w_2 f_2, \tag{10}$$

where

$$f_1 = \int_D \left(\frac{1}{2}\mu \sum_{i,j} \left(\frac{\partial u_i}{\partial x_j} + \frac{\partial u_j}{\partial x_i} \right)^2 + \mu \sum_i \alpha(\gamma)\, u_i^2 \right) \mathrm{d}\Omega, \tag{11}$$

and

$$f_2 = \int_{\Gamma_b} T \mathrm{d}\Omega. \tag{12}$$

Here, w_1 and w_2 are weighting factors, which balance the thermal-fluid performance of the optimized designs. By adjusting w_1 and w_2 settings, the multi-objective performance can be explored.

D. Optimization Formulation

The overall optimization formulation is summarized as follows:

$$\begin{aligned} \underset{\phi}{\text{minimize:}} \quad & f(\gamma), \\ \text{subject to:} \quad & \phi \in [-1,1]^D, \\ & \text{design variable regularization}, \\ & \text{physics equilibrium}, \end{aligned} \tag{13}$$

where ϕ is the nodal design variable ranging between -1 and 1. The regularization procedure, $\phi \rightarrow \gamma$, utilizes the prior expressions (3) and (4). The weighted objective function, $f(\gamma)$, is provided in (10) to (12). The governing equations for conjugate heat transfer are detailed in (5) to (9). A notable omission in the optimization formulation is the often-used volume fraction constraint. Here, the volume fraction of the optimized design is naturally determined based on the choice of weighting factors in the multi-objective function, (10).

E. Numerical Implementation

The governing equations for conjugate heat transfer physics explained in Section II-B are solved using COMSOL commercial software using a finite element method. The iterative update of the design variable, ϕ, is performed in MATLAB using the method of moving asymptotes [38]. The sensitivity analysis follows the standard adjoint method, which is implemented in COMSOL with automatic differentiation. The COMSOL-MATLAB Livelink is used to communicate between the two computing platforms. While the optimization is performed using the porous media approach, all TO designs reported in this paper have been post-processed with separately modeled fluid and solid domains. Accordingly, a Boolean operation is used to appropriately model the surface boundary between the resulting fluid and solid domains. Such post-processing is necessary to guarantee accurate numerical analysis by avoiding any fluid seepage into the solid domain.

III. Numerical Results

This section presents a numerical case study, which compares the thermal-fluid performance of MMC heat sinks using conventional straight rectangular fins versus MMC heat sink designs obtained using TO fin/channel geometries. The overall cold plate assembly design follows the image presented in Fig. 1. For simplicity here, all designs assume an identical manifold insert component, although it is logical that the manifold may eventually be merged into the overall optimization strategy.

Material properties are summarized in Table I with copper for the solid and 50/50 water/ethylene-glycol for the fluid. Fluid is supplied at the inlet for the entire cold plate at a constant flow rate of 0.25 l/min at a fixed temperature of 338.15 K. The base plate is uniformly heated with heat flux of 100 W/cm^2. The overall fin area is prescribed as 36 mm $\times$ 36 mm. The base plate thickness is 2 mm. The manifold insert component has 8 dividers, 4 inlets and 4 outlets. To manage the computational cost, a unit cell model is used for the analysis and design optimization. The unit cell length is 4.5 mm (along the rectangular fin direction). The unit cell width is 1.8 mm (along the manifold divider direction). As a result, the total number of unit cells is 160. Symmetry boundary conditions are applied to all four sides of the unit cell; refer to Fig. 3.

TABLE I
Material properties

Property	Symbol	Value	Unit
Fluid density	ρ	1003.5	kg/m^3
Fluid dynamic viscosity	μ	0.00065	Pa $\cdot$ s
Fluid thermal conductivity	k_f	0.4267	W/(m $\cdot$ K)
Fluid specific heat capacity	C_p	3662.2	J/(kg $\cdot$ K)
Solid thermal conductivity	k_s	400	W/(m $\cdot$ K)

A. Conventional Rectangular Fins

As a baseline, the thermal-fluid performance of MMC heat sinks with conventional straight rectangular fins is analyzed.

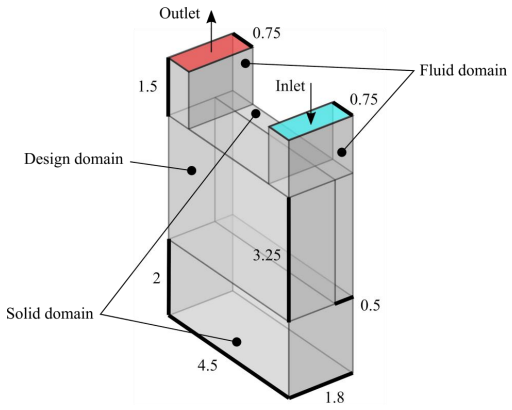

Fig. 3. Unit cell design domain and boundary condition settings for TO.

The fin/channel width ratio within the unit cell is varied, and Fig. 4 presents four sampled designs. As seen in the steady-state temperature contours of the solid domain and fluid streamlines, both the maximum temperature of the base plate and the temperature at the fluid outlet decrease as the fluid channel becomes narrower. Simultaneously, the fluid velocity through the channel itself increases. Thus, the thermal performance increases for narrower channels, and performance is characterized by the average temperature difference, ΔT, between the base plate temperature and the fluid inlet temperature. On the other hand, narrower channel designs also experience an attendant increase in pressure drop indicating inferior fluid performance. Specifically, for the same volumetric flow rate, higher pressure drop requires more pumping power for any heat sink system. Detailed thermal-fluid performance of the four sampled designs is summarized in Fig. 5.

B. TO Designed Fin/Channel Geometries

The design domain and boundary conditions again follow Fig. 3 for the TO study. The design domain is meshed with 230640 hexahedral elements. The adopted design variable regularization scheme often guarantees the mesh independence of the optimized results. The fluid domain minimum feature size is governed by the filter radius R_ϕ. However, the feature size is not explicitly controlled for the solid domain in the current formulation. A more comprehensive mesh independence study is left as future work. The unit cell dimensions are identical to those used in Section III-A. Here, it is noted that a solid wall of 0.5 mm thickness is prescribed in the unit cell to guarantee the appropriate support of the insert component and to model the periodic nature of the design. Fluid enters and exits the unit cell vertically with prescribed fluid domains based on the insert geometry. Thus, the TO design domain is a 4.5 mm $\times$ 1.3 mm $\times$ 3.25 mm cuboid that allows free-form distribution of either solid (*i.e.*, walls) or fluid (*i.e.*, channels).

Three TO designs with different prescribed weighting factors (w_1 and w_2) are presented in Fig. 6. Each design is converged in 150 optimization iterations. One solver call (*i.e.*, coupled laminar flow plus heat conduction and convection) is required per optimization iteration. Non-intuitive geometries are generated, which are otherwise extremely challenging to obtain via an empirical design process. As the ratio of w_2/w_1 increases, the optimized design favors heat transfer performance over fluid flow performance. It is also observed that a larger volume fraction of solid material generally leads to better thermal performance. This is due to an increase of the wetted surface area of the design and an increase in more

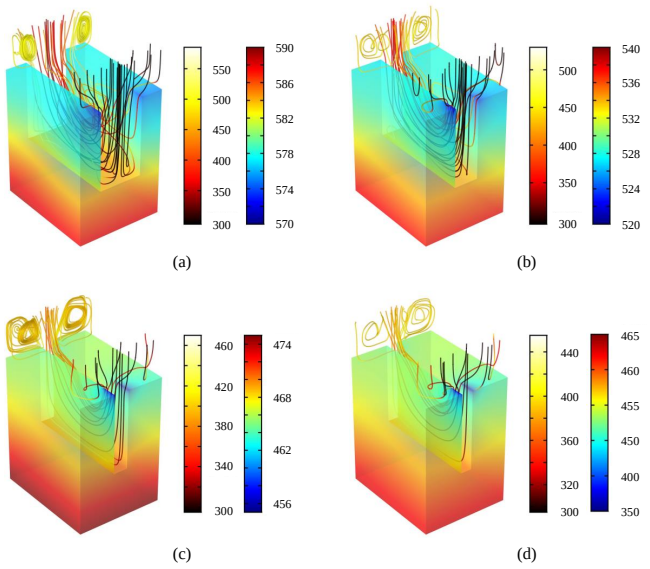

Fig. 4. Unit cell analysis of conventional MMC heat sinks with straight rectangular fins. Four designs with variable ratios of channel and wall widths are presented. Channel widths are (a) 1.8 mm; (b) 1.0 mm; (c) 0.6 mm and (d) 0.45 mm. Colored solid domains indicate temperature distributions corresponding to the right color bar in all sub-figures. Colored streamlines indicate the coolant flow path and temperature; refer to the left color bar in each sub-figure. Color bar temperature units: K.

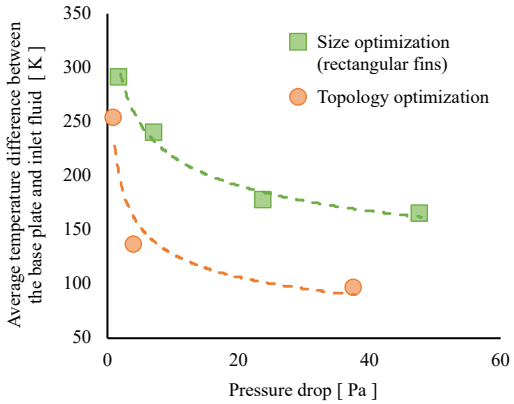

Fig. 5. Thermal-fluid performance comparison between TO designed MMC heat sinks and conventional MMC heat sinks. The thermal performance is measured by the average temperature difference between the base plate and inlet fluid (Y-axis). The fluid performance is measured by the pressure drop between inlet and outlet (X-axis).

conductive solid material. However, as the volume fraction of the solid material increases, the pressure drop also tends to increase due to the narrowed and more tortuous flow path. This trade-off agrees with the trend observed for conventional MMC heat sinks with straight microchannels (Section III-A). Detailed thermal-fluid performance of the three TO designs are summarized in Fig. 5. For the sake of demonstration, Fig. 7 presents the entire MMC heat sink using the TO designed fin/channel unit cell geometry of Fig. 6(b).

C. Performance Comparison

As shown in Fig. 5, the thermal-fluid performance of TO designs outperform that for the conventional designs with straight rectangular fins. At a given pressure drop, the TO designs provide a lower average temperature of the base plate. Likewise, to achieve the same cooling performance, the TO designs require less pumping power. This result is due to an enhanced wetted surface area, as well as, a flow path that is more contoured to the overall u-shaped coolant flow trajectory through the unit cell. Additionally, for the designs that have higher heat transfer performance, the generation of additional pin-fin-like structures further disrupts the thermal boundary layer, thus enhancing fluid mixing and lowering the base plate average temperature. Uniquely, these pin-fin-like features are not only attached to the bottom wall of the design domain, but also appear on the fin sidewalls of the design domain, as well.

Note that the results presented in Fig. 5 only explore design variations within a fixed unit cell size. For the case of straight channel designs, it is further assumed that only a single channel is allowed per unit cell, which leads to a fixed number of channels in the heat sink. However, it is expected that as the number of straight channels increases, the thermal-fluid performance curve will change accordingly. Nonetheless, the discovery that TO designs outperform straight channel designs is likely valid for any given unit cell dimensions.

IV. Conclusion

This article presented a TO method for designing novel 3-D MMC heat sink fin/channel geometries. The conjugate heat transfer governed geometry exploration problem was formulated using a density-based TO method and solved by gradient-based optimization. The numerical results demonstrated that, in a prescribed unit cell domain, TO designs outperformed conventional designs with straight rectangular fins. The thermal performance was measured by the average difference between the base plate temperature and the inlet fluid temperature (*i.e.*, inversely proportional to the heat transfer coefficient with fixed heat flux). The fluid performance was quantified using the pressure drop (*i.e.*, proportional to the required pumping power). Such designs may exploit the tremendous fabrication flexibility afforded by state-of-the-art additive manufacturing; for example, a representative additively fabricated TO MMC heat sink design is shown in Fig. 8. Future work follows related research [33] and includes the experimental validation of TO MMC heat sink designs fabricated using additive manufacturing.

References

[1] D. B. Tuckerman and R. F. W. Pease, "High-performance heat sinking for vlsi," *IEEE Electron device letters*, vol. 2, no. 5, pp. 126–129, 1981.

[2] W. Qu and I. Mudawar, "Flow boiling heat transfer in two-phase micro-channel heat sinks—-i. experimental investigation and assessment of correlation methods," *International journal of heat and mass transfer*, vol. 46, no. 15, pp. 2755–2771, 2003.

[3] R. Chein and J. Chuang, "Experimental microchannel heat sink performance studies using nanofluids," *International Journal of Thermal Sciences*, vol. 46, no. 1, pp. 57–66, 2007.

[4] G. M. Harpole and J. E. Eninger, "Micro-channel heat exchanger optimization," in *1991 Proceedings, Seventh IEEE Semiconductor Thermal Measurement and Management Symposium*. IEEE, 1991, pp. 59–63.

[5] D. Copeland, M. Behnia, and W. Nakayama, "Manifold microchannel heat sinks: isothermal analysis," in *InterSociety Conference on Thermal Phenomena in Electronic Systems, I-THERM V*. IEEE, 1996, pp. 251–257.

[6] W. Escher, T. Brunschwiler, B. Michel, and D. Poulikakos, "Experimental investigation of an ultrathin manifold microchannel heat sink for liquid-cooled chips," *Journal of Heat Transfer*, vol. 132, no. 8, p. 081402, 2010.

[7] C. S. Sharma, S. Zimmermann, M. K. Tiwari, B. Michel, and D. Poulikakos, "Optimal thermal operation of liquid-cooled electronic chips," *International Journal of Heat and Mass Transfer*, vol. 55, no. 7-8, pp. 1957–1969, 2012.

[8] Y. Yue, S. K. Mohammadian, and Y. Zhang, "Analysis of performances of a manifold microchannel heat sink with nanofluids," *International Journal of Thermal Sciences*, vol. 89, pp. 305–313, 2015.

[9] M. P. Bendsøe and N. Kikuchi, "Generating optimal topologies in structural design using a homogenization method," *Computer Methods in Applied Mechanics and Engineering*, vol. 71, no. 2, pp. 197–224, 1988.

[10] M. P. Bendsøe, "Optimal shape design as a material distribution problem," *Structural and multidisciplinary optimization*, vol. 1, no. 4, pp. 193–202, 1989.

[11] G. I. Rozvany, M. Zhou, and T. Birker, "Generalized shape optimization without homogenization," *Structural and Multidisciplinary Optimization*, vol. 4, no. 3, pp. 250–252, 1992.

[12] Y. M. Xie and G. P. Steven, "A simple evolutionary procedure for structural optimization," *Computers & structures*, vol. 49, no. 5, pp. 885–896, 1993.

[13] M. Y. Wang, X. Wang, and D. Guo, "A level set method for structural topology optimization," *Computer methods in applied mechanics and engineering*, vol. 192, no. 1-2, pp. 227–246, 2003.

[14] G. Allaire, F. Jouve, and A.-M. Toader, "Structural optimization using sensitivity analysis and a level-set method," *Journal of computational physics*, vol. 194, no. 1, pp. 363–393, 2004.

[15] T. Borrvall and J. Petersson, "Topology optimization of fluids in stokes flow," *International journal for numerical methods in fluids*, vol. 41, no. 1, pp. 77–107, 2003.

[16] P. I. Borel, A. Harpøth, L. H. Frandsen, M. Kristensen, P. Shi, J. S. Jensen, and O. Sigmund, "Topology optimization and fabrication of photonic crystal structures," *Optics Express*, vol. 12, no. 9, pp. 1996–2001, 2004.

[17] T. Nomura, K. Sato, K. Taguchi, T. Kashiwa, and S. Nishiwaki, "Structural topology optimization for the design of broadband dielectric resonator antennas using the finite difference time domain technique," *International Journal for Numerical Methods in Engineering*, vol. 71, no. 11, pp. 1261–1296, 2007.

[18] M. B. Dühring, J. S. Jensen, and O. Sigmund, "Acoustic design by topology optimization," *Journal of sound and vibration*, vol. 317, no. 3-5, pp. 557–575, 2008.

[19] M. P. Bendsøe and O. Sigmund, *topology optimization theory, methods, and applications*. Springer, 2004.

[20] E. M. Dede, "Multiphysics topology optimization of heat transfer and fluid flow systems," in *proceedings of the COMSOL Users Conference*, 2009.

[21] G. H. Yoon, "Topological design of heat dissipating structure with forced convective heat transfer," *Journal of Mechanical Science and Technology*, vol. 24, no. 6, pp. 1225–1233, 2010.

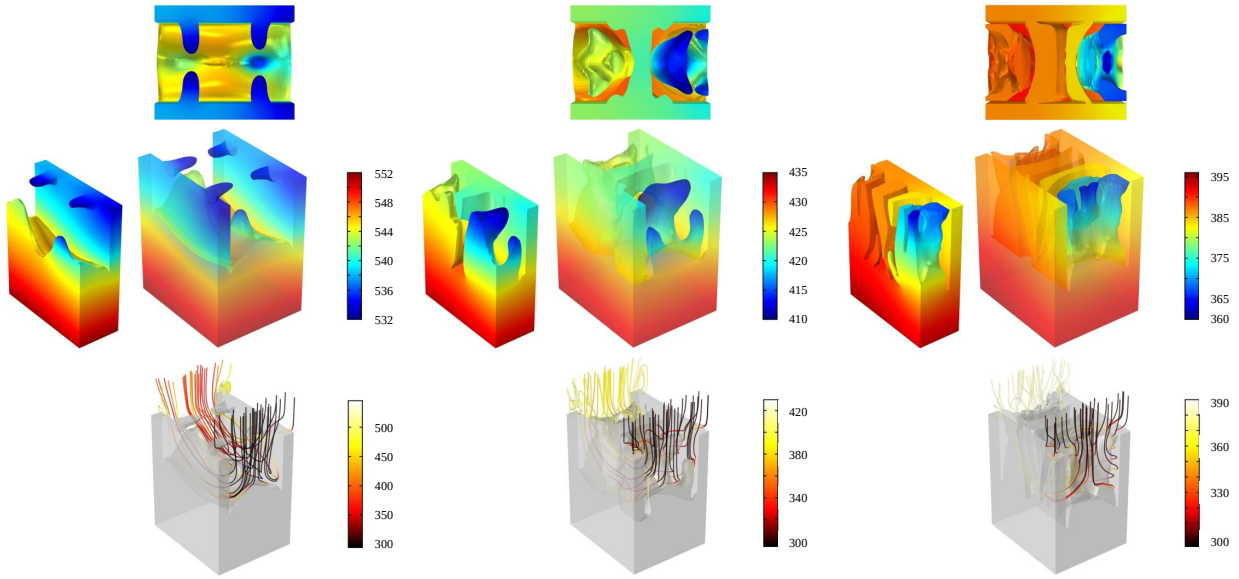

Fig. 6. TO designed MMC heat sink unit cell geometries with variable ratios of multi-objective weighting factors. Weighting factor ratios w_2/w_1 are (a) 0.33; (b) 2 and (c) 100. Colored solid domains indicate temperature distributions. Colored streamlines indicate the coolant flow path and temperature. Color bar temperature units: K.

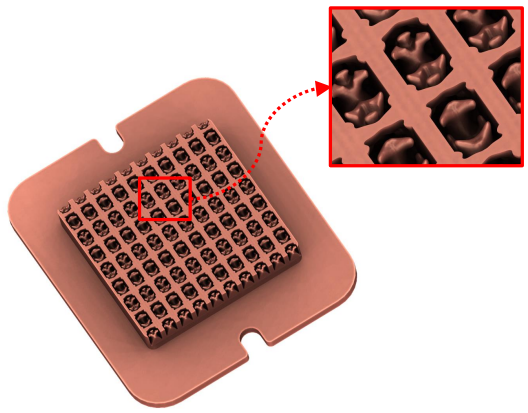

Fig. 7. An MMC heat sink model with the example TO designed fin/channel unit cell geometry of Fig. 6(b).

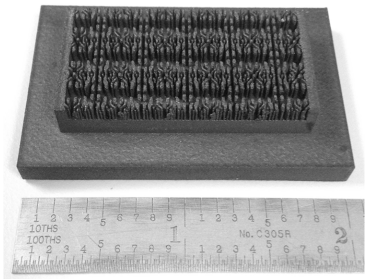

Fig. 8. A representative additively fabricated TO MMC heat sink design.

[22] E. M. Dede, S. N. Joshi, and F. Zhou, "Topology optimization, additive layer manufacturing, and experimental testing of an air-cooled heat sink," *Journal of Mechanical Design*, vol. 137, no. 11, p. 111403, 2015.

[23] J. Alexandersen, O. Sigmund, and N. Aage, "Large scale three-dimensional topology optimisation of heat sinks cooled by natural convection," *International Journal of Heat and Mass Transfer*, vol. 100, pp. 876–891, 2016.

[24] J. Alexandersen, O. Sigmund, K. E. Meyer, and B. S. Lazarov, "Design of passive coolers for light-emitting diode lamps using topology optimisation," *International Journal of Heat and Mass Transfer*, vol. 122, pp. 138–149, 2018.

[25] E. M. Dede, "Optimization and design of a multipass branching microchannel heat sink for electronics cooling," *Journal of Electronic Packaging*, vol. 134, no. 4, p. 041001, 2012.

[26] T. Matsumori, T. Kondoh, A. Kawamoto, and T. Nomura, "Topology optimization for fluid–thermal interaction problems under constant input power," *Structural and Multidisciplinary Optimization*, vol. 47, no. 4, pp. 571–581, 2013.

[27] A. A. Koga, E. C. C. Lopes, H. F. V. Nova, C. R. De Lima, and E. C. N. Silva, "Development of heat sink device by using topology optimization," *International Journal of Heat and Mass Transfer*, vol. 64, pp. 759–772, 2013.

[28] K. Yaji, T. Yamada, S. Kubo, K. Izui, and S. Nishiwaki, "A topology optimization method for a coupled thermal–fluid problem using level set boundary expressions," *International Journal of Heat and Mass Transfer*, vol. 81, pp. 878–888, 2015.

[29] S. Zeng and P. S. Lee, "Topology optimization of liquid-cooled microchannel heat sinks: An experimental and numerical study," *International Journal of Heat and Mass Transfer*, vol. 142, p. 118401, 2019.

[30] S. Yan, F. Wang, J. Hong, and O. Sigmund, "Topology optimization of microchannel heat sinks using a two-layer model," *International Journal of Heat and Mass Transfer*, vol. 143, p. 118462, 2019.

[31] M. Pietropaoli, F. Montomoli, and A. Gaymann, "Three-dimensional fluid topology optimization for heat transfer," *Structural and Multidisciplinary Optimization*, vol. 59, no. 3, pp. 801–812, 2019.

[32] S. Sun, P. Liebersbach, and X. Qian, "Large scale 3d topology optimization of conjugate heat transfer," in *2019 18th IEEE Intersociety Conference on Thermal and Thermomechanical Phenomena in Electronic Systems (ITherm)*. IEEE, 2019.

[33] S. N. Joshi, Z. Yu, H. Sennoun, J. Hampshire, and E. M. Dede, "Single-phase cooling performance of a topology optimized and additively-

manufactured multi-pass branching microchannel heat sink," in *2020 19th IEEE Intersociety Conference on Thermal and Thermomechanical Phenomena in Electronic Systems (ITherm)*. IEEE, 2020.

[34] B. S. Lazarov and O. Sigmund, "Filters in topology optimization based on Helmholtz-type differential equations," *International Journal for Numerical Methods in Engineering*, vol. 86, no. 6, pp. 765–781, 2011.

[35] A. Kawamoto, T. Matsumori, S. Yamasaki, T. Nomura, T. Kondoh, and S. Nishiwaki, "Heaviside projection based topology optimization by a PDE-filtered scalar function," *Structural and Multidisciplinary Optimization*, vol. 44, no. 1, pp. 19–24, 2011.

[36] L. H. Olesen, F. Okkels, and H. Bruus, "A high-level programming-language implementation of topology optimization applied to steady-state navier–stokes flow," *International Journal for Numerical Methods in Engineering*, vol. 65, no. 7, pp. 975–1001, 2006.

[37] J. Alexandersen, N. Aage, C. S. Andreasen, and O. Sigmund, "Topology optimisation for natural convection problems," *International Journal for Numerical Methods in Fluids*, vol. 76, no. 10, pp. 699–721, 2014.

[38] K. Svanberg, "The method of moving asymptotes—a new method for structural optimization," *International Journal for Numerical Methods in Engineering*, vol. 24, no. 2, pp. 359–373, 1987.